Gas Detectors

DOI: 10.1002/anie.200700314

Noble Gases Influence the Conductance of Cetineite-Type Nanoporous Semiconductors**

*Dorota Sendor, Boniface P. T. Fokwa, Richard Dronskowski, and Ulrich Simon**

Cetineites are oxoselenoantimonates with zeolite-like channel structures. Academic, as well as technical, interest in these materials derives from the combination of their nanoporous nature and photosemiconducting properties, which was once unique for the entire class of inorganic nanoporous solids.[1] In the meantime, the group of microporous and nanoporous semiconductors has been extended by other zeolite analogues.[2] We have already reported the synthesis, electronic structure, and electrical conductivity of cetineites.[1,3] Conductivity measurements on pressed pellets of polycrystalline samples at room temperature gave the first hints that even weakly interacting gases, such as noble gases and nitrogen, could influence the conductance of cetineites.[4] This finding is extraordinarily interesting and unique, because typically only the adsorption of oxidizing or reducing gases affects the concentration and mobility of the charge carriers of oxide semiconductors at higher temperatures, leading to a change in conductance.

The selective adsorption and storage of noble gases is of both fundamental and technological interest.[5–7] The investigation of these processes requires the precise determination of the adsorption sites, as most recently reported for the adsorption of Ar and N_2 in the structurally related metal–organic frameworks (MOFs).[8,9] However, the finding that noble-gas adsorption may cause a reversible change in the electrical properties of such a material, while the host lattice retains its structural integrity, composition, and high symmetry, is entirely new.

Herein, we show that the electronic conductance of the cetineite $K_6[Sb_{12}O_{18}][SbSe_3]_2{\cdot}7H_2O$ (referred to hereafter as K;Se) is reversibly influenced by the adsorption of He, Ne, Ar, Kr, and Xe. We first optimized the hydrothermal synthesis of K;Se to obtain single crystals large enough both to perform electrical-transport measurements under different gas atmospheres and to determine the adsorption sites of the noble gases by single-crystal X-ray diffraction (XRD). The general composition of cetineites is $A_6[Sb_{12}O_{18}][SbX_3]_2{\cdot}(7-mx-y)H_2O{\cdot}x(B^{m+}(OH)_m){\cdot}y\square$ (abbreviated as: A;X; $A^{a+} = = Na^+$, K^+, Rb^+, Ba^{2+}, Sr^{2+}; $X = S^{2-}$, Se^{2-}; $B^{m+} = Na^+$, Sb^{3+}; $\square$ symbolizes an unoccupied lattice site).[10] The structure contains one-dimensional tubelike structural units with a diameter of approximately 7 Å, which consist of $\{SbO_3\}$ pyramids linked by common oxygen atoms. Isolated $[SbX_3]^{3-}$ pyramids are located between the tubes. The electrically neutral tubes are held together by predominantly ionic bonds between the A^{a+} ions lining the inner walls of the tubes and the chalcogen atoms of the isolated $[SbX_3]^{3-}$ pyramids (Figure 1). The host lattice can, and easily does, accept a number of guest molecules. A common guest species is molecular water in association with the B^{m+} and OH^- ions. We have repeatedly shown that, only in the case of K;Se, some of the water molecules contained inside the tubes can be reversibly removed at room temperature under high vacuum.[5] Therefore, we concentrated on K;Se in the optimization of the synthesis and the subsequent investigations.

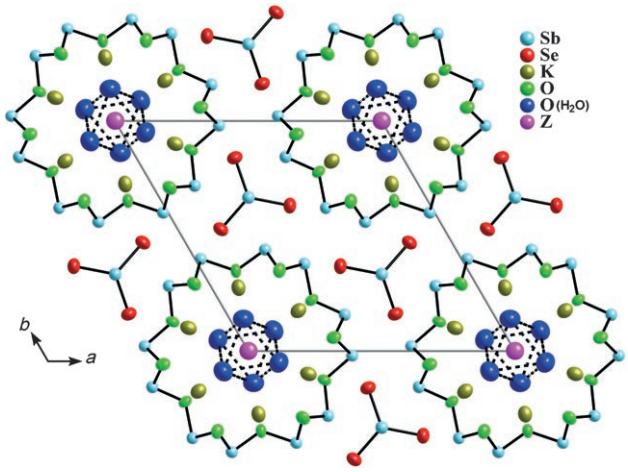

Figure 1. Projection of the structure of K;Se along the [001] axis. $Z = H_2O$, He, Ne, Ar, Kr, or Xe. Displacement ellipsoids are drawn at the 90% probability level.

The crystals of K;Se were synthesized under hydrothermal conditions, as described in Ref. [1]. To perform conductance measurements parallel to the crystallographic *c* axis, contacts were applied to the crystals with silver paint. To keep the (001) plane free of silver paint, one contact was applied to one end of the needle-like crystal, and the second contact was applied to the side of the crystal right below the opposite end. This approach allowed the tubes to be accessed by gases. After evacuation for 15 min at 10^{-5} mbar, the

[*] Dr. D. Sendor, Dr. B. P. T. Fokwa, Prof. Dr. R. Dronskowski, Prof. Dr. U. Simon
Institute of Inorganic Chemistry
RWTH Aachen University
52056 Aachen (Germany)
Fax: (+49) 241-809-9003
E-mail: ulrich.simon@ac.rwth-aachen.de

[**] We thank Claudia Klöser for the synthesis of the cetineites, Manfred Speldrich for help with the vacuum equipment, and Klaus Kruse for collecting the single-crystal diffraction data. D.S. gratefully acknowledges the Alexander von Humboldt Foundation (Roman Herzog-Forschungsstipendium) for the financial support of this work.

crystals were charged with the guest species (from a compressed-gas cylinder) at a pressure of up to 1 bar. Between the individual sorption phases, the sample space was re-emptied by evacuation. We carefully monitored the dehydration using thermogravimetry (TG) coupled with mass spectroscopy (MS). In an Ar atmosphere, water desorbs from K;Se in two steps (Figure 2). The first step occurs at about 290 °C with

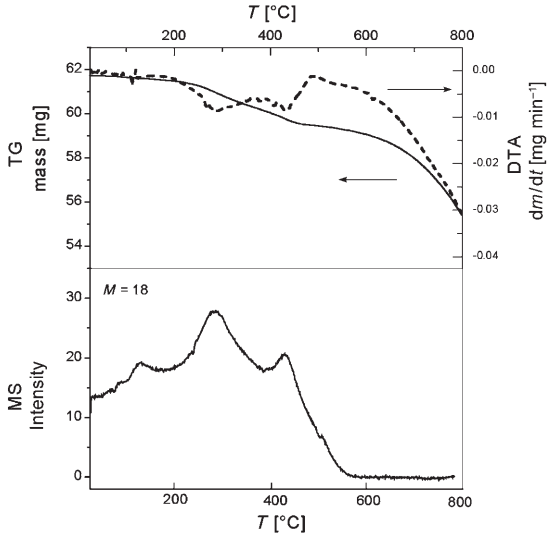

Figure 2. Thermogravimetry (TG) and differential thermal analysis (DTA) coupled with mass spectrometry (MS) of K;Se.

a weight loss of 0.75 %. The second step, which is associated with the maximum desorption, occurs at about 490 °C (and has a high-temperature tail up to 520 °C) with a weight loss of 3.50 %. From these findings, we conclude that the water molecules at the Z position in Figure 1 are desorbed at 290 °C, while those located in octahedral symmetry around the Z site remain inside the structure up to 490 °C, owing to their stronger binding to the host lattice. However, the water desorption at higher temperatures is associated with a gradual decomposition of the material. Thus, the complete removal of water can only be achieved by careful heating at temperatures significantly below 400 °C under vacuum. Furthermore, we noted that the ease and degree of desorption can vary widely for different crystals. We assume that, in some cases, structural defects may hinder the desorption of water.

The electrical resistance (R) of K;Se was measured during the adsorption/desorption cycles of He, Ne, Ar, Kr, and Xe at room temperature under illumination with white light. The sensitivity ($S = (R_{gas} - R_{vacuum})/R_{vacuum}$) and the response time (τ_{50}) were investigated (Table 1). Figure 3 a shows the resistance of a single crystal of K;Se, measured during the adsorption/desorption cycles of Ne, Ar, Xe, and He. After each adsorption phase, the sample chamber was evacuated. In all the adsorption cycles, the resistance of K;Se increases significantly in the presence of the guest species. The sensitivity of the response depends almost linearly on the atomic radius (r_A) of the guest species (Figure 3 b). The median response time (τ_{50}; the time needed to reach 50 % of the final signal) was determined experimentally from the saturation of the change in resistance after the test gas was applied. As for the sensitivity, the mean response time also decreases with increasing atomic radius.

Table 1: Median response time (τ_{50}) and sensitivity (S) for single crystals of K;Se loaded with different noble gases.

Noble gas	r_A [pm]	τ_{50} [s]	S
He	128	25	0.420 ± 0.044
Ne	140	38	0.326 ± 0.043
Ar	174	62	0.275 ± 0.021
Kr	190	64	0.213 ± 0.037
Xe	218	70	0.172 ± 0.032

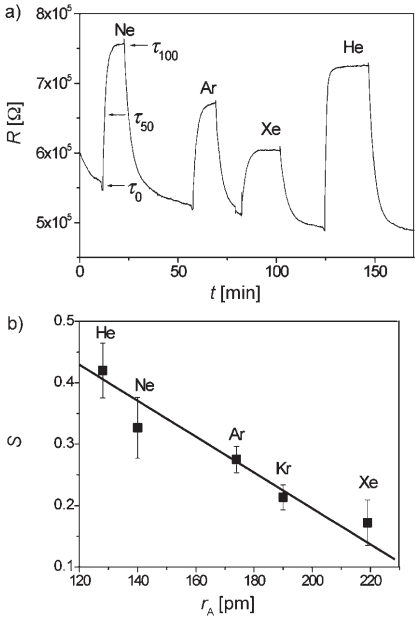

Figure 3. a) Change in resistance (R) during the sorption/desorption cycles of different noble gases in a single crystal of K;Se. b) Dependence of the sensitivity (S) on the atomic radius (r_A) of the noble gases. See text for details.

To better understand these experimental findings, we analyzed the adsorption sites of the gas species by using the same single crystals and experimental conditions as described above. The crystals were mounted in capillaries connected to a gas manifold. After evacuation, the capillaries were filled with Xe, Kr, Ar, Ne, or He gas and then flame sealed. We first carried out single-crystal structure analyses on non-evacuated single crystals. The crystal structures were solved in space group $P6_3/m$ (no. 176) by direct methods[11] and refined by full-matrix least-squares methods (on F^2).[12] The atomic positions were then standardized with the program STRUCTURE TIDY.[13] Our analyses showed the presence of very weak superstructure reflections, as previously observed for K;Se by Wang and Liebau.[14] However, the intensities of these reflections were too weak for a full data collection; thus, our structure refinements had to be based on the averaged substructure. Nonetheless, we found that the structure of K;Se contains one water molecule more (at the Z position at the corner of the unit cell; Figure 1) than the previously

reported phase.[14] Note that all the selected single crystals showed the presence of this water molecule, which is located in an octahedral void (Wyckoff position 2*b* at 0,0,0; refined occupancy 0.49(5); largest electron-density peak and hole 1.08 and $-1.08\,e\,Å^{-3}$) surrounded by the six other water molecules.

Since the thermogravimetric investigations on this phase revealed two desorption steps for water, the first at 290 °C and the second at 490 °C (Figure 2), it was assumed that, in the first step, the water molecule at the octahedral 2*b* site (Z) is desorbed. To verify this hypothesis, the single crystals were heated at 100 °C under vacuum at 10^{-5} mbar (the same conditions used for the conductance experiments above), and single-crystal XRD data were collected. The refinement of these data confirmed the retention of the hexagonal symmetry of the averaged structure of K;Se, and the absence of a water molecule at the 2*b* site (largest electron-density peak and hole 1.15 and $-1.03\,e\,Å^{-3}$). Moreover, the electron density at Wyckoff site 2*b* is only $0.85\,e\,Å^{-3}$ (Figure 4, left), indicating the absence of any guest atom at this site.

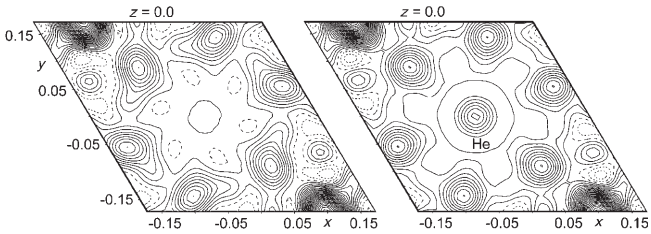

Figure 4. Two-dimensional electron-density maps (F_{obs}) around the 2*b* site at 0,0,0, plotted from the single-crystal XRD data collected for an evacuated single crystal of K;Se (left) and for a He-loaded single crystal of K;Se (K;Se·δHe; right). The unit cells are projected along the [001] axis ($-0.5 \le z \le 0.5$). The dashed lines are negative contours; the contour lines are spaced by $5\,e\,Å^{-3}$.

We also performed the same experiments on other cetineites but were unable to remove the different guest species (H_2O, OH^-, and B^{m+}) in these cases. The presence of water rather than B^{m+} in the octahedral 2*b* site is very likely the reason for the different sorption behavior of K;Se compared to the other known cetineites.

The evacuated single crystal of K;Se was then filled with Xe, and a new set of XRD data was collected. A small expansion of the lattice parameters was found (from 14.581(3) and 5.607(2) Å to 14.600(3) and 5.610(2) Å, corresponding to a small, but significant, volume increase of 3.2(4) $Å^3$), indicating that the amount of Xe adsorbed was also small. The structure model of the evacuated crystal of K;Se was used for the refinement of the Xe-containing crystal (K;Se·δXe). *R* values of under 5 % were achieved, but a peak appeared in the difference Fourier map exactly at Wyckoff site 2*b* (about $4\,e\,Å^{-3}$, compared to $0.85\,e\,Å^{-3}$ for the evacuated crystal). The position was assigned to an Xe atom, and subsequent refinements led to even better *R* values and to an Xe content of only 0.050(8) per formula unit; the largest electron-density peak and hole remaining in the difference Fourier map were 1.03 and $-1.51\,e\,Å^{-3}$, respectively.

Different single crystals were used for the same procedure of evacuation and filling with other noble gases. The refinements of the XRD data sets collected converged only when the occupancies of the noble-gas atoms (Xe, Kr, Ar, or Ne) were freely refined with all atoms having anisotropic displacement parameters. Only in the case of He did the refinement converge with a full occupancy of the 2*b* site (Figure 4, right), but the displacement parameter of the very light He atom was refined isotropically.[12] The refined noble-gas content per formula unit (δ) decreases with increasing atomic radius (Table 2): 2.0 for He, 0.24(6) for Ne, 0.16(2) for Ar, 0.084(8) for Kr, and 0.050(8) for Xe. This result corresponds very well with the results of the electrical-conductance measurements, where a decrease in the change in resistance (that is, the sensitivity) with increasing size of the noble gas is also observed (Figure 3b).

Table 2: Lattice parameters, *R* values, and refined noble-gas content per formula unit (δ) for single crystals of K;Se·δZ.

	a [Å]	*c* [Å]	R_1, wR_2 ($I > 2\sigma(I)$)	Data/Parameters	δ
K;Se	14.581(3)	5.607(2)	0.030, 0.073	606/49	
K;Se·δHe	14.592(3)	5.610(2)	0.030, 0.080	606/51	2.0
K;Se·δNe	14.601(2)	5.609(1)	0.036, 0.069	606/51	0.24(6)
K;Se·δAr	14.578(2)	5.608(2)	0.031, 0.073	747/51	0.16(2)
K;Se·δKr	14.594(3)	5.605(2)	0.026, 0.066	606/51	0.084(8)
K;Se·δXe	14.600(3)	5.610(2)	0.033, 0.068	606/51	0.050(8)

In summary, we have shown that the cetineites are an exciting class of materials having photoconduction properties that depend on the presence of guest molecules within the tubes of the host lattice. Although the degree of loading and the storage capability of K;Se are rather low compared to those of other materials, such as MOFs,[16] the reversible change in conductance enables the detection of noble gases.

Experimental Section

In a typical synthesis of K;Se, Sb (0.38 g), Se (0.37 g), and KOH (0.4 g) were mixed with water (1.3 g) and 2-aminopentane (0.25 mL). The mixture was transferred into a teflon-coated autoclave and heated at 200 °C for 4 days. The reaction product was washed with water and dried at room temperature in air. Because, in some cases, the (001) faces of the crystals were capped by an amorphous oxide layer, the ends of the crystals had to be broken off for the conductance measurements.

The direct current (dc) through the crystals was measured by applying a constant voltage of 10 V using an electrometer (Keithley 6517). The measurements showed that cetineites are poor conductors in the dark, having an almost linear current–voltage relationship. Irradiation with white light results in an increase in conductance. The dc conductance (*G*) and resistance (*R*) were deduced directly from the measured current at 10 V, according to Ohm's law.

The thermogravimetry was performed on a Mettler Toledo 851e instrument in the range 25–800 °C at a rate of $10\,°C\,min^{-1}$ in Ar.

The XRD data were collected using a single-crystal diffractometer (Enraf Nonius CAD4) at room temperature, and the intensities

were corrected for absorption using a numerical procedure.[15] Further details on the crystal structure investigations may be obtained from the Fachinformationszentrum Karlsruhe, 76344 Eggenstein-Leopoldshafen, Germany (fax: (+49) 7247-808-666; e-mail: crysdata@fiz-karlsruhe.de), on quoting the depository numbers CSD-416761 (K;Se·H_2O), CSD-416762 (K;Se), CSD-416763 (K;Se·δHe), CSD-416764 (K;Se·δNe), CSD-416765 (K;Se·δAr), CSD-416766 (K;Se·δKr), and CSD-416767 (K;Se·δXe).

Received: January 23, 2007
Revised: May 20, 2007
Published online: July 19, 2007

Keywords: electrical conductance · nanoporous materials · noble gases · semiconductors · X-ray diffraction

[1] U. Simon, F. Schüth, S. Schunk, X. Wang, F. Liebau, *Angew. Chem.* **1997**, *109*, 1138; *Angew. Chem. Int. Ed. Engl.* **1997**, *36*, 1121.
[2] See, for example: A. E. C. Palmqvist, B. B. Iversen, E. Zanghellini, M. Behm, G. D. Stucky, *Angew. Chem.* **2004**, *116*, 718; *Angew. Chem. Int. Ed.* **2004**, *43*, 700; A. Shulman, A. E. C. Palmqvist, *Angew. Chem.* **2007**, *119*, 732; *Angew. Chem. Int. Ed.* **2007**, *46*, 718.
[3] F. Starrost, E. E. Krasovskii, W. Schattke, J. Jockel, U. Simon, X. Wang, F. Liebau, *Phys. Rev. Lett.* **1998**, *80*, 3316; U. Simon, J. Jockel, F. Starrost, E. E. Krasovskii, W. Schattke, *Nanostruct. Mater.* **1999**, *12*, 447.
[4] F. Starrost, E. Krasowskii, W. Schattke, J. Jockel, U. Simon, R. Adelung, L. Kipp, M. Skibowski, *Phys. Rev. B* **2000**, *61*, 15697.
[5] F. Laeri, F. Schüth, U. Simon, M. Wark, *Host–Guest Systems Based on Nanoporous Crystals*, Wiley-VCH, Weinheim, **2003**, pp. 451–477.
[6] H. Li, M. Eddaoudi, M. O'Keeffe, O. M. Yaghi, *Nature* **1999**, *402*, 276.
[7] H. K. Chae, D. Y. Siberio-Pérez, J. Kim, Y. Go, M. Eddaoudi, A. J. Matzger, M. O'Keeffe, O. M. Yaghi, *Nature* **2004**, *427*, 523.
[8] Y. Kubota, M. Takata, R. Matsuda, R. Kitaura, S. Kitagawa, K. Kato, M. Sakata, T. C. Kobayashi, *Angew. Chem.* **2005**, *117*, 942; *Angew. Chem. Int. Ed.* **2005**, *44*, 920.
[9] J. L. C. Rowsell, E. C. Elinor, J. Eckert, J. A. K. Howard, O. M. Yaghi, *Science* **2005**, *309*, 1350.
[10] X. Wang, F. Liebau, *Eur. J. Solid State Inorg. Chem.* **1998**, *35*, 27.
[11] G. M. Sheldrick, SHELXS-97, Program for the solution of crystal structures, Universität Göttingen **1997**.
[12] G. M. Sheldrick, SHELXL-97, Program for the refinement of crystal structures, Universität Göttingen **1997**.
[13] L. M. Gelato, E. Parthé, *J. Appl. Crystallogr.* **1987**, *20*, 139.
[14] X. Wang, F. Liebau, *Z. Kristallogr.* **1999**, *214*, 820.
[15] W. R. Busing, H. A. Levy, *Acta Crystallogr.* **1957**, *10*, 180; P. Coppens, L. Leiserowitz, D. Rabinovich, *Acta Crystallogr.* **1965**, *18*, 1035.
[16] U. Müller, M. Schuber, F. Teich, H. Puetter, K. Schierle-Arndt, J. Pasté, *J. Mater. Chem.* **2006**, *16*, 626.

